Relationship between Helium Transport and Molecular Motions in a Glassy Polycarbonate

Andrei A. Gusev and Ulrich W. Suter*

Institut für Polymere, ETH Zentrum, CH-8092 Zürich, Switzerland

David J. Moll

Central Research of Dow Chemical Company, Building 1702, Midland, Michigan 48674

Received September 14, 1994
Revised Manuscript Received January 17, 1995

Introduction. The technological relevance of the transport of gas molecules through dense polymers has become evident in recent years through steadily increasing practical applications, such as gas-separation membranes and barrier materials.[1] However, despite the manifest increase in technological demand, there has been a considerable lack of understanding of the microscopic fundamentals underlying solubility and diffusion of even the smallest molecules. Among other unanswered questions has been the relationship between solute transport and molecular motions in polymer matrices.

Recent molecular dynamics (MD) studies[2] have demonstrated that, on time scales up to nanoseconds that are accessible today with MD, the motion of gas molecules in bulk polymers is coupled to the fast thermal vibration of the polymer atoms but is not facilitated by the structural rearrangements occurring in the matrices on this time scale (for example, rotational flips of methyl groups). Naturally, this important observation cannot straightforwardly be carried over to longer times where other molecular motions, such as the rotational motion of phenylene rings in Bisphenol A polycarbonate (BPA-PC), could contribute to the solute transport.

In this paper we shall present experimental and simulation data on helium transport in glassy BPA-PC. The data were collected over the temperature range from 100 to 300 K (T_g of BPA-PC is ca. 450 K) and elucidate the extent to which various molecular motions in the BPA-PC matrix contribute to the transport of helium molecules.

Experimental Section. The experimental permeation data were obtained using Bisphenol A polycarbonate prepared via interfacial polymerization with a resulting $M_w = (31 \pm 1) \times 10^3$. Films of 30–40 μm thickness were obtained by casting a solution of polycarbonate in methylene chloride onto a glass plate. After slow evaporation, the remaining residual solvent was removed by placing the samples in a vacuum oven for more than 15 h at 100 °C.

The films were mounted in an aluminum permeation cell containing a sintered stainless steel porous frit for support. The films were sealed within the permeation cell with Viton O-rings that defined an active area for permeation of 11.4 cm^2. The permeation cell was mounted in a closed-cycle helium refrigerator cryostat. The cell temperature was maintained by a proportional-integrator cryostat that operated a resistive heater.

Pure helium gas (99.999%) was applied to the feed side of the membrane at pressures between 2 and 5 bar. The permeating gas was directed to a vacuum chamber pumped by a 170 L/s turbomolecular pump. The chamber contained a Balzers QM9064 quadrupole mass spectrometer. Permeation gas flow rates were determined by comparing measured mass spectrometer ion currents from permeation with currents measured for commercially available helium-calibrated leaks. Ion current signals for permeation and the calibrated leaks were corrected for background signals.

Permeabilities were calculated from permeation flow rates, the film area and thickness, and the applied feed-gas pressure. Diffusivities were determined by the time-lag method where the permeation flow rate is monitored as a function of time after the feed gas is applied. The diffusivity was calculated using $D = 0.139L^2/t_{1/2}$ where L is the film thickness and $t_{1/2}$ is the time required for the permeation value to reach half the steady-state permeation rate.[3]

Modeling Section. Microstructures. In these calculations, we used three atomistically explicit microstructures, each consisting of one BPA-PC chain of 75 repeat units packed in a cubic cell of ca. 30 Å, employing the *pcff* force field.[4] The creation of the microstructures was started at a density of 0.8 g/cm^3. The cells were subjected[5] to 170 ps of constant temperature–pressure MD[6] with itegration steps of 1 fs, at three different temperatures—110, 175, and 300 K—followed by energy minimization with a conjugate-gradient method until the maximum atomic gradient became less than 10^{-3} kcal/Å. A cutoff distance of 8.5 Å was used for the nonbonded interactions. In order to account for the finite cutoff, a tail-correction pressure of 1600 bar was imposed on the microstructures in dynamics. Every 10^3 steps of integration took about 1 h of CPU time on a Silicon Graphics Crimson workstation. The densities of the minimized cells agreed, within a percent or so, with the experimental densities of BPA-PC. The coordinates of the polymer atoms in the minimized cells were used for the calculation of transport properties of helium in BPA-PC by means of the transition state approach (TSA).[7]

Transition State Approach (TSA). The TSA explicitly assumes that (i) small molecules move in polymer matrices by thermally activated jumps and (ii) on the time scales relevant for the solute transport the polymer atoms only elastically fluctuate about certain average positions. In this situation, the behavior and properties of the solute can be described[7] with a time-independent single-particle distribution function $\varrho(\boldsymbol{r})$, where $\boldsymbol{r}$ is the location, thus allowing for modeling the transport of small solutes in solids on time scales far beyond the reach of MD.

It was demonstrated[7] that the simplest isotropic homogeneous approximation to the elastic motion of the polymer atoms is suitable in understanding the fundamentals of the transport of small molecules. Within this approximation, the thermal fluctuations of the position of all polymer atoms are described by the isotropic Gaussian functional form with one and the same mean-square deviation $\langle\Delta^2\rangle$. The appropriate value of the smearing factor $\langle\Delta^2\rangle$ can be determined either from MD trajectories of the polymer matrix or from results of X-ray or neutron scattering from polymers and is on the order of 0.1 Å^2 at ambient conditions.

The technicalities involved in evaluating $\varrho(\boldsymbol{r})$ and carrying out the simulation of the solute dynamics on the network of local maxima of $\varrho(\boldsymbol{r})$ have already been discussed in detail elsewhere.[2,7]

Results and Discussion. The smearing factor $\langle\Delta^2\rangle$ of the microstructures was evaluated from the last 20 ps of the MD trajectories. Figure 1 shows that the thermal motion of polymer atoms becomes stationary

0024-9297/95/2228-2582$09.00/0

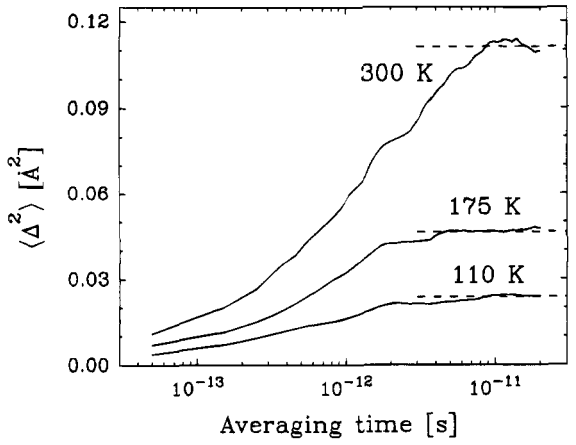

Figure 1. Elastic fluctuations of the polymer atoms in the microstructures of BPA-PC. The stationary values shown by the horizontal dashed lines are taken for the calculations of transport properties of helium molecules in BPA-PC.

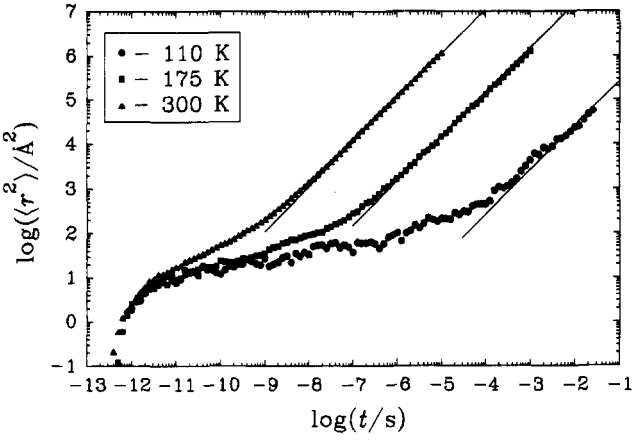

Figure 2. Dynamics of helium molecules in the cells of BPA-PC. Symbols at 300 and 175 K show averages over 1500 random walks (500 walks in each of the three microstructures) and symbols at 110 K over 150 random walks. Solid lines with slope 1 exactly represent the Einstein diffusive mode $\langle r^2\rangle = 6Dt$. The onset of Einstein diffusion occurs at several dozen angstroms; this is about the size of the microstructures used. Unfortunately, the present computer resources do not permit the generation of microstructures sufficiently large to unambiguously elucidate the extent to which finite size effects are operative.

on the time scale of picoseconds; we used the level-off values of $\langle\Delta^2\rangle$ for evaluating the helium distribution function $\varrho(\boldsymbol{r})$. In short MD control runs we found that switching off the thermostat did not change the level-off values of $\langle\Delta^2\rangle$, while switching off the manostat (going from *NPT* to *NVT* dynamics) brought about a decrease of ca. 10% in the $\langle\Delta^2\rangle$ values. This change did not influence significantly the results discussed below.

Figure 2 depicts the calculated time dependence of the mean-square displacement $\langle r^2\rangle$ of helium molecules in the BPA-PC microstructures. On the time scale of the individual solute jumps, i.e., a few picoseconds (see Figure 3), we observe temperature-independent local mobility. The helium molecules then follow anomalous dynamics with $\langle r^2\rangle \propto t^n$ ($n < 1$). At long times, the helium dynamics becomes diffusive with $\langle r^2\rangle = 6Dt$, where D is the diffusion coefficient. The permeability coefficient P was evaluated via $P = DS$, where the solubility coefficient S was calculated through normalization of the solute distribution function $\varrho(\boldsymbol{r})$.[7,8]

Figures 4 and 5 show that both the diffusivity and

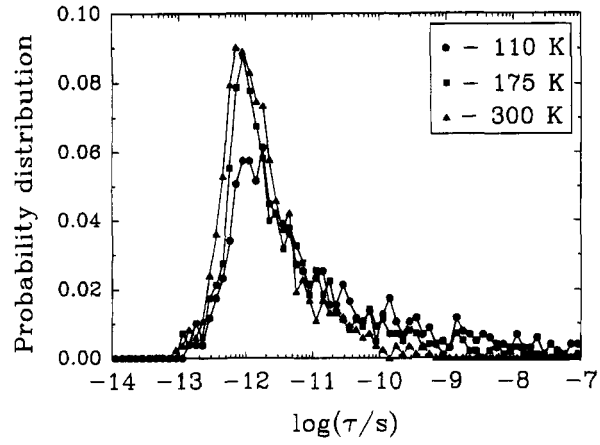

Figure 3. Distribution of residence times of helium molecules in the local maxima of $\varrho(\boldsymbol{r})$ as calculated in the microstructures of BPA-PC.

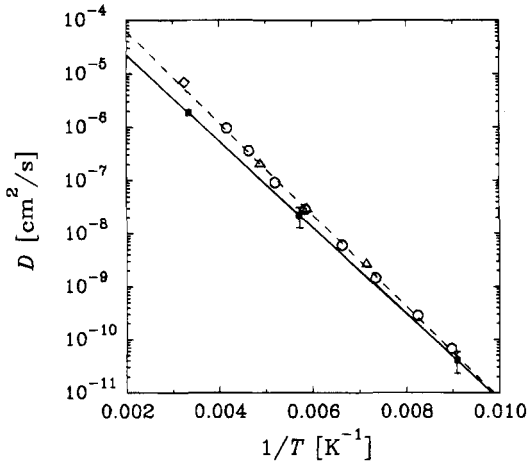

Figure 4. Diffusivity of helium in BPA-PC. Hollow symbols represent experimental data: circles, sample 1; triangles, sample 2; diamond, ref 9. Filled squares with error bars represent predicted data averaged at each temperature over three microstructures. The dashed line fits experimental data, and the solid line fits calculated data.

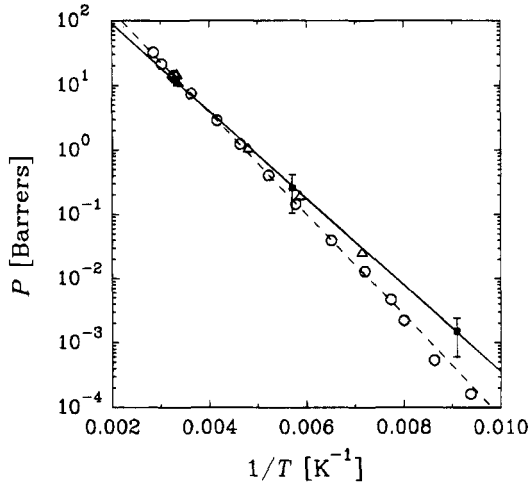

Figure 5. Permeability of helium in BPA-PC. See Figure 3 for symbol specification. 1 barrer = 1×10^{-10} cm^3(STP)·cm/(cm^2·s·cmHg).

permeability data can be fitted with the Arrhenius form over the entire temperature range of about 200 K studied. From this we conclude that the mechanism of helium transport in glassy BPA-PC is the same for all temperatures studied.

Table 1. Experimental and Calculated Activation Energies (in kcal/mol) of Diffusion and Permeability Coefficients of Helium Transport in BPA-PC[a]

	E_a(exp)	E_a(calc)	E_a^T	E_a^ϱ	E_a^Δ
D	3.9	3.7	1.4	0.2	2.0
P	3.5	3.2	0.9	0.3	1.9

[a] To evaluate E_a^T, we used the microstructures produced at 300 K and calculated their transport properties at 300 and 175 K with the value of $\langle\Delta^2\rangle$ obtained at 300 K. The values of E_a^ϱ were evaluated by taking the microstructures produced at 300 and 175 K and calculating D and P with $T = 300$ K and the value of $\langle\Delta^2\rangle$ obtained at 300 K. For the evaluation of E_a^Δ we employed the microstructures produced at 300 K, $T = 300$ K, and the value of $\langle\Delta^2\rangle$ obtained at 300 and 175 K.

Within the model there are three factors which determine the temperature dependence of the diffusion and permeability coefficients: the ("diffusant") temperature T, the density ϱ, and the smearing factor $\langle\Delta^2\rangle$. Accordingly, the apparent activation energy can be decomposed into three contributions stemming from these factors (here given for D only):

$$E_a \equiv -\frac{d(\log D)}{d(1/T)} = -\frac{\partial(\log D)}{\partial(1/T)} - \frac{\partial(\log D)}{\partial\varrho}\frac{\partial\varrho}{\partial(1/T)} - \frac{\partial(\log D)}{\partial\langle\Delta^2\rangle}\frac{\partial\langle\Delta^2\rangle}{\partial(1/T)} = E_a^T + E_a^\varrho + E_a^\Delta$$

Table 1 shows that for both the diffusion and permeability coefficients the smearing factor $\langle\Delta^2\rangle$ accounts for more than 50% of the total E_a. It is surprising that the density contribution is so small compared to the other two factors.

The TSA neglects any coupling between the solute transport and molecular motions in the polymer matrix apart from the fast elastic vibration of polymer atoms. Nevertheless, in the absence of adjustable parameters, the predicted and experimental data are in quite good agreement. This fact convinces us that we are dealing with a physically correct model of the helium transport and that it is the fast elastic vibration of the polymer atoms which is exclusively relevant: All other motions in the glassy BPA-PC matrix appear to be too slow to affect the helium transport.

References and Notes

(1) Spillman, R. W. *Chem. Eng. Prog.* **1989**, *85*, 14.
(2) For a review, see: Gusev, A. A.; Müller-Plathe, F.; van Gunsteren, W. F.; Suter, U. W. *Adv. Polym. Sci.* **1994**, *116*, 207.
(3) Felder, R. M. *J. Membr. Sci.* **1978**, *3*, 15.
(4) Sun, H.; Mumby, S. J.; Maple, J. R.; Hagler, A. T. *J. Am. Chem. Soc.*, in press.
(5) InsightII and Discover3.1, 1993, Biosym Technologies, Inc., San Diego, CA.
(6) Berendsen, H. J. C.; Postma, J. P. M.; van Gunsteren, W. F.; DiNola, A.; Haak, J. R. *J. Chem. Phys.* **1984**, *81*, 3684.
(7) (a) Gusev, A. A.; Arizzi, S. A.; Moll, D. J.; Suter, U. W. *J. Chem. Phys.* **1993**, *99*, 2221. (b) Gusev, A. A.; Suter, U. W. *J. Chem. Phys.* **1993**, *99*, 2228.
(8) Gusev, A. A.; Suter, U. W. *Phys. Rev.* **1991**, *A43*, 6488.
(9) Muruganandam, N.; Koros, W. J.; Paul, D. R. *J. Polym. Sci., Polym. Phys. Ed.* **1987**, *25*, 1999.

MA945083G